

Low-complexity Base Station Selection Scheme in mmWave Cellular Networks

Christodoulos Skouroumounis, *Student Member, IEEE*, Constantinos Psomas, *Member, IEEE*, and Ioannis Krikidis, *Senior Member, IEEE*

Department of Electrical and Computer Engineering,

University of Cyprus, Cyprus

Email: {cskour03, psomas, krikidis}@ucy.ac.cy

Abstract

In this paper, we study the performance of next-generation cellular networks in the context of a low complexity base station (BS) selection scheme. In contrast to existing BS cooperation approaches, where multiple BSs jointly transmit to the user, by using our proposed low-complexity technique, a user communicates with the BS that provides the maximum signal-to-interference-plus-noise-ratio from a set formed according to a pre-selection policy. We consider three pre-selection policies based on: 1) the Euclidean distance, 2) the averaged received power, and 3) a random selection. Moreover, we consider the case where the users have the ability to employ the successive interference cancellation (SIC) scheme. Despite its high computational complexity, SIC can potentially decode and remove strong interfering signals from the aggregate received signal which can significantly boost the user's performance. By using stochastic geometry tools, analytical expressions for the coverage performance are derived for each policy, by taking into account spatial randomness and blockage effects. Our proposed technique provides low computational and implementation complexity due to the two-level selection scheme. Furthermore, we show that our proposed scheme does not lose in diversity compared to existing cooperation techniques and that all policies can benefit by the employment of the SIC scheme.

Index Terms

BS coordination, heterogeneous networks, mmWave, sectorized antennas, successive interference cancellation.

Preliminary results of this work were presented at the IEEE Global Communications Conference, Washington, DC, Dec. 2016 [1].

I. INTRODUCTION

The wireless industry is currently facing the barrier of limited available spectrum for commercial cellular systems and an increasing demand of data traffic. During the past decades, much effort has been made to enhance network throughput. Different advanced communication techniques, such as multiple-input multiple-output techniques and interference coordination have been fully exploited in wireless networks to provide high spectral efficiency [2]. Furthermore, the employment of millimeter wave (mmWave) bands (30-300 GHz) along with the deployment of denser networks, is becoming a promising option to support extremely high data rates and higher spectral efficiency.

MmWave communications have fundamental differences with the current sub-6 GHz cellular networks in terms of propagation losses and sensitivity to blockages. Due to their band nature, higher frequency signals are more susceptible to atmospheric absorption, deflection and diffraction [3], resulting in higher propagation losses. In addition, due to the poor ability of signals to penetrate objects, mmWave networks are unsuitable for outdoor environments without employing techniques that compensate the limitations of those signals [4]. These characteristics of mmWave communications pose several challenges to fully exploit their potentials. On the other hand, the short wavelength used in mmWave frequencies leads to the placement of a large number of miniaturized antennas with highly directional beam gain in order to combat the high path loss [5]. Additionally, one of the key advantages of mmWave communication technology is the large amount of spectral bandwidth available. By exploiting the wide available bandwidth, mmWave wireless links can achieve high capacities, which is unlikely to be matched by any lower frequency wireless technologies.

The ultra-dense deployment of small cells in multi-tier heterogeneous networks, provides a fundamental way to meet the capacity demands of next-generation wireless networks. The network densification has been investigated as a potential solution for increasing the spectral efficiency, motivated by the need of reducing the link's distance between the transmitter and the receiver. By bringing the transmitters closer to the receivers, the link quality can be enhanced due to the significantly reduced propagation losses [6]. However, the deployment of additional base stations (BSs), increases the multi-user interference in the network [7]. As a result, the high level of interference in a denser network is the most important obstacle for successful connectivity. Motivated by the need of interference control to further enhance the performance

of denser networks, recent studies show an ascending interest for effective interference mitigation techniques.

In order to address the aforementioned issues, techniques such as the cooperative transmission of BSs, the directionality of the network's antennas and interference mitigation techniques are considered. An efficient approach to combat inter-cell interference is to exploit the cooperation among the multiple randomly located BSs from different network tiers via a high-capacity backhaul link. Therefore, with the use of BS cooperation, the user exploits the benefits of distributed multiple antenna systems, and hence the network throughput increases [8]. Furthermore, aiming to mitigate the high path losses imposed by mmWave signals, directional antennas can be employed. Specifically, with the use of larger antenna arrays, mmWave cellular systems can implement beamforming at the transmitter and the receiver, providing array gains that compensate mmWave high path-losses, overcome additional noise power, and reduce out-of-cell interference. Finally, due to the additional interference caused by the network densification, effective interference mitigation techniques are investigated. The ability of the users to potentially decode the strong interfering signals and remove them from the aggregate received signal, leads to a significant improvement in network performance. The cooperation between BSs in ultra-dense mmWave cellular networks, employing directional antennas and the successive interference cancellation (SIC) scheme, can enable Gb/s-level access speeds with less spectrum usage and lower power consumption [9].

Past Work: An efficient technique for increasing the network performance, is the cooperation among interconnected distributed BSs. Although the cooperation between BSs has been extensively studied for conventional communication systems, its deployment in high frequency bands under the presence of blockages has only recently been investigated. In [10], the authors investigate a non-coherent joint transmission BS cooperative scheme and characterize the performance from a system-level standpoint. In [11], a heterogeneous cellular network where each user is served by a number of nearby single-antenna BSs to mitigate inter-cell interference is considered. The work in [12], studies the negative effects of blockages and analyze the coverage performance for cellular networks by using tools from random shape theory. A low-complexity BS cooperation technique is proposed in [13], and the network performance is evaluated for scenarios with channel state information (CSI) at the transmitter. This work is further extended in [1], where the authors show that the low-complexity BS cooperation technique based on the averaged received power, ensures full diversity gain. The performance of mmWave cellular networks using a

channel model that incorporates blockage effects was proposed in [14], where it is shown that the achievable rate in mmWave networks can outperform microwave cellular networks by an order-of-magnitude. Current research has shown that the point-to-point systems using mmWave can achieve high data rates, while reducing interference over long distance [15]. In [16], the authors develop a geometry-based stochastic channel model for outdoor environments and study the effect of all the first-order reflection paths between the transmitter and the receiver. The authors in [17], provide a comprehensive overview of mathematical models and analytical techniques for mmWave cellular systems. Finally, a mmWave heterogeneous network that mitigates multi-user interference through sophisticated BS cooperative techniques is studied in [18].

Aiming to increase the link gains which will further boost the network performance, directional antennas are employed. Beamforming is a well investigated technology for conventional communication systems [19]–[21], nevertheless, its deployment for high frequency bands under the presence of blockages has only recently been investigated. Specifically, due to the inherently directional mmWave signals, the use of directional antennas can provide higher link gains [22]. The work in [23], shows that the use of directional antennas at each node of a mmWave communication network along with the use of signals that are inherently directional, reduces the received interference and supports higher densities and larger spectral efficiencies. The authors in [24], study mmWave cellular networks and show that sectorized antennas can provide significant gains. In [25], the authors investigate the potential benefits of the directional beamforming in mmWave cellular networks and show that by increasing the main lobe gain results in higher coverage performance probability. The authors in [26], study the importance of using the actual antenna pattern in the coverage analysis for mmWave networks.

On the other hand, the need for better network performance, has motivated the study of more sophisticated techniques for multi-user interference mitigation [27], [28]. A SIC policy is investigated in [29], [30], where the authors evaluate the performance after successfully decoding and canceling the most dominant interfering signals. The deployment of this method in heterogeneous networks was investigated in [31], where it is shown that the main additional gain can be achieved through the cancellation of the strongest interfering signal. In [32], the authors study the employment of a SIC scheme in heterogeneous networks and show that the performance benefits decrease with the number of cancellations.

Contribution: In this paper, we study the downlink performance of a heterogeneous mmWave cellular network where antenna directionality is employed. We adopt a system-level point of

view by taking into account both BS and blockage spatial randomness. Specifically, the main contributions of this paper are as follows:

- We propose a BS selection scheme that is based on a two-level procedure: in the first-level, a set of “candidate” BSs is defined and at the second-level, the user selects from this set the BS which provides the highest signal-to-interference-plus-noise-ratio (SINR). The proposed two-level BS selection technique reduces the signaling and thus is attractive for practical and low-complexity implementations.
- We evaluate the achieved performance of our proposed technique in the context of two popular and well investigated BS selection policies. Specifically, the pre-selection is based either on the Euclidean distance or the averaged received signal power. For comparison purposes, we also investigate our proposed technique with a random BS selection policy.
- We investigate the employment of an ideal SIC method for the downlink in mmWave cellular networks to further emphasize the achieved network performance using the proposed technique. With the intention to keep low computational complexity, we assume that the user eliminates only its dominant interferer without depriving from the network to achieve better coverage performance.
- Finally, analytical and asymptotic expressions are derived for the coverage probability for each pre-selection policy by employing Nakagami fading. In addition, analytical expressions of the coverage probability for the case where the users have the ability to perform SIC are also provided for the scenarios considered. These closed-form expressions provide a quick and convenient methodology of evaluating the system’s performance and obtaining insights into how key system parameters affect the performance.

Our results demonstrate that our proposed scheme does not lose in diversity compared to coordinated multi-point (CoMP) technique and also outperforms it. Furthermore, our results illustrate the negative effects of blockages both on the network performance and the diversity order. Also, our results reveal that the pre-selection policy based on the averaged received signal power, outperforms in terms of achieved coverage performance from the other two pre-selection policies. Finally, we show that with the employment of SIC, the observed interference from the user is significantly reduced, providing a noticeable increase to the user’s performance at low to moderate target threshold.

Paper Organization: Section II introduces the network model together with the channel,

blockage and sectorized antenna models. In Section III, the pre-selection policies are presented. The low-complexity BS selection scheme is proposed in Section IV, and the performance along with the asymptotic expressions for Nakagami fading are evaluated. In Section V, we consider the case where the users perform the SIC scheme for the special case of Rayleigh fading. Simulation results are presented in Section VI, followed by our conclusions in Section VII.

Notation: \mathbb{R}^d denotes the d -dimensional Euclidean space, $\|x\|$ denotes the Euclidean norm of $x \in \mathbb{R}^d$, $\mathbb{P}[X]$ denotes the probability of the event X and $\mathbb{E}[X]$ represent the expected value of X , $\binom{n}{k} = \frac{n!}{k!(n-k)!}$ is the binomial coefficient and $\Gamma[a]$ and $\Gamma[a, x]$ denote the complete and upper incomplete gamma functions, respectively.

II. SYSTEM MODEL

In this section, we provide details of the considered system model; the main mathematical notation related to the system model is summarized in Table I. The network is studied from a large-scale point of view using stochastic geometry. Consider a heterogeneous cellular network composed by K network tiers of BSs. We assume the BSs are connected by an ideal backhaul network, which provides the ability to the BSs from different tiers to cooperate and jointly transmit data to a user [23]. Each network tier $k \in \{1, \dots, K\}$ of BSs is modeled by a two-dimensional homogeneous Poisson Point Process (PPP) Φ_k with density λ_k .

A. Channel and blockage model

We assume that all the BSs that belong to the network tier $k \in \{1, \dots, K\}$, transmit with the same power P_k . We assume independent Nakagami fading for each link. Different parameters of Nakagami fading ν_L and ν_N are assumed for line-of-sight (LOS) and non-LOS (NLOS) links and so the power of the channel fading depending on the link's status, $\ell \in \{L, N\}$, is a normalized Gamma random variable with shape parameter ν_ℓ and scale parameter $1/\nu_\ell$. Furthermore, we assume all wireless links exhibit additive white Gaussian noise with zero mean and variance σ^2 . The path-loss model is given by the expression $\|x - y\|^{-a}$ which assumes that the received power decays with the distance between the transmitter x and the receiver y , where $a > 2$ denotes the path loss exponent. Throughout this paper, we will denote by r_u the distance from BS u to the origin i.e., $r_u = \|u\|$.

TABLE I: Summary of Notations

Notation	Description	Notation	Description
K	Total number of tiers	$\gamma = \{\gamma_1^*, \dots, \gamma_K^*\}$	Normalized path-losses of “candidate” BSs
Φ_k	PPP of tier $k \in \{1, \dots, K\}$	$\mathbf{r} = \{r_{u_1^*}, \dots, r_{u_K^*}\}$	Distances of “candidate” BSs
λ_k	Density of PPP Φ_k	ν_L, ν_N	LOS, NLOS Nakagami fading parameter
P_k	Transmit power of k -th tier BS	$\mathcal{P}_L, \mathcal{P}_N$	Probability of link in LOS, NLOS
$\ell \in \{L, N\}$	Link’s status (LOS, NLOS)	p_G	Probability of link gain equal to G
a_L, a_N	LOS, NLOS path-loss exponent	$\Pi \in \{CS, SS, RS\}$	Pre-selection policy
r_{u_k}	Distance between origin and point u in tier k	G, G_0	Interfering and direct link gain
$\gamma_k = r_{u_k}^{a_\ell} / P_k$	Normalized path-loss	\mathcal{C}^Π	“Candidate” BSs set for policy Π
$\Psi_k = \left\{ \frac{r_v^{a_\ell}}{P_k}, v \in \Phi_k \right\}$	PPP with normalized path-losses	$\lambda_i^\Pi(r), \lambda_i^\Pi(\gamma)$	Intensity of Φ_i and Ψ
$r_{u_k^*}, \gamma_k^*$	Distance, normalized path-loss to “candidate” BS	$f_\Phi^\Pi(\mathbf{r}), f_\Psi^\Pi(\gamma)$	Joint distribution of \mathbf{r} and γ

The blockages are modeled by a line segment process of two dimensional lines with random lengths and orientations. Under such a scenario, it was shown that the probability of a communication link to be LOS is [12]

$$\mathcal{P}_L = \mathbb{P}[LOS] = \exp(-\beta r), \quad (1)$$

where r denotes the distance between the receiver and the transmitter and β is a non-negative blockage constant that models the blockage density and their characteristics [12]. Under the assumption that the BSs are modeled as points of a homogeneous PPP and that the events that the BS-to-user links are either in LOS or NLOS are independent, Φ can be partitioned into two independent and non-homogeneous PPPs i.e., Φ^L and Φ^N , such that $\Phi = \Phi^L \cup \Phi^N$. This originates from the thinning property of the PPPs [33] The LOS and NLOS links have different path-loss exponents, a_L and a_N , respectively, and are the same for all network tiers. Hence, the path-loss exponent $a(r)$ for the link between a BS located at distance r from a user, is modeled as a discrete random variable described by

$$a(r) = \begin{cases} a_L & \text{with probability } \mathcal{P}_L, \\ a_N & \text{with probability } \mathcal{P}_N = 1 - \mathcal{P}_L, \end{cases} \quad (2)$$

where \mathcal{P}_L is given by expression (1).

B. Sectorized antenna model

We assume the employment of multiple transmit/receive antennas at both the BSs and the users. Adaptive directional beamforming is assumed to be employed at each terminal (BS or user) and is modeled as in [23]. To simplify the analysis, we make use of the approximation of

an actual beam pattern using a sectorized model. Both the transmit and receive beam patterns are parameterized by three values: the gain of a link between the receiver and the transmitter is parameterized by three values: main lobe beamwidth $\theta \in [0, 2\pi]$, main lobe gain M , and side lobe gain m [23]. The gain of an interference link seen by the user, is a discrete random variable described by

$$G = \begin{cases} M^2 & \text{with probability } p_{M^2} = \left(\frac{\theta}{\pi}\right)^2, \\ Mm & \text{with probability } p_{Mm} = 2\left(\frac{\theta}{\pi}\right)\left(\frac{\pi-\theta}{\pi}\right), \\ m^2 & \text{with probability } p_{m^2} = \left(\frac{\pi-\theta}{\pi}\right)^2, \end{cases} \quad (3)$$

where p_G is the probability of a link to have gain equal to $G = \{M^2, Mm, m^2\}$. We assume the active link between each user and its associated BS lies in the boresight direction of the antennas of both terminals, resulting in a link gain of M^2 , denoted by G_0 .

III. LOW COMPLEXITY BS SELECTION TECHNIQUE

Our proposed BS selection scheme is based on a two-level procedure. Initially, in the first-level phase, the set of K “candidate” BSs is pre-selected, without taking into consideration the fading channel factor. The set of the “candidate” BSs for each user, consists of the pre-selected BSs with which the user is able to communicate. Specifically, according to the rules of the adopted pre-selection policy, from each network tier $k \in \{1, \dots, K\}$, a single BS is selected. The set defined by the pre-selected BSs from all network tiers, represents the set of “candidate” BSs to establish connectivity with their associated user, $\mathcal{C} \subset \bigcup_{k=1}^K \Phi_k$. At the second-level phase, the user selects from the K “candidate” BSs, the one which provides the highest SINR, while the rest of the “candidate” BSs are ignored. Due to the pre-selection of the K “candidate” BS, our proposed selection scheme requires channel estimation for only K links instead of $\sum_{k=1}^K N_k$ links, where N_k is a Poisson random variable denoting the number of BSs in tier k . In addition, the low complexity of the proposed technique stems from the fact that users connect to a single BS, opposed to the jointly BS transmission technique of the conventional approaches, that demands higher computation complexity. **This is where the novelty of our proposed technique is highlighted. Particularly, by applying the proposed technique, the complexity of implementing BS cooperation in heterogeneous mmWave network can be significantly decreased.**

In the following sections, the three pre-selection policies are presented and the set of “candidate” BSs for each policy is derived.

A. Closest LOS pre-selection policy (CS)

Firstly, we consider the case where the set of “candidate” BSs to communicate with their associated user, consists of the closest LOS BS from each network tier; Fig. 1a schematically depicts the CS policy. The CS policy requires an a priori knowledge of the location of the BSs. This knowledge can be obtained by monitoring the location of the BSs through a low-rate feedback channel or by a global positioning system mechanism. The CS policy does not take into account the instantaneous fading resulting in a low implementation complexity, specifically for scenarios with low mobility. In this case, the set \mathcal{C}_{CS} is defined as

$$\mathcal{C}_{\text{CS}} = \left\{ u_k^* : u_k^* = \arg \max_{u \in \Phi_k} r_u^{-1}, k \in \{1, \dots, K\}, r_u \in \Phi^{\text{L}} \right\}. \quad (4)$$

B. Strongest pre-selection policy (SS)

For the second pre-selection policy, we consider the case where the set of “candidate” BSs to communicate with their associated user, consists of the BS that provides the strongest received signal power from each network tier; Fig. 1b schematically depicts the SS policy. Along with the information regarding the BS location, the SS policy also requires the transmit power of the BSs. Similarly as before, this can be obtained through a low-rate feedback channel. This case is applicable to wireless networks, where users keep a list of the neighboring BSs with the strongest averaged received signal power to initiate handoff requests. We define the set of “candidate” BSs for this policy as

$$\mathcal{C}_{\text{SS}} = \left\{ u_k^* : u_k^* = \arg \max_{u \in \Phi_k} \frac{P_k}{r_u^{a(r_u)}}, k \in \{1, \dots, K\} \right\}. \quad (5)$$

Note that in the case where the transmit power of the BSs of all tiers is the same, the SS policy selects the BSs with the smallest path loss from each network tier k .

C. Random pre-selection policy (RS)

As a third pre-selection policy, we consider the case where the set of “candidate” BSs, consists of a randomly selected BS that is located inside a disk of radius R around its associated user, from each network tier k ; Fig. 1c depicts the RS policy. The pre-selection of a random BS from network tier k is independent of whether the communication link with its associated user is LOS or NLOS. In the case where there is not any available BS inside the disk of radius R , the user is in outage. The RS policy does not require any feedback about the location of the BSs and so

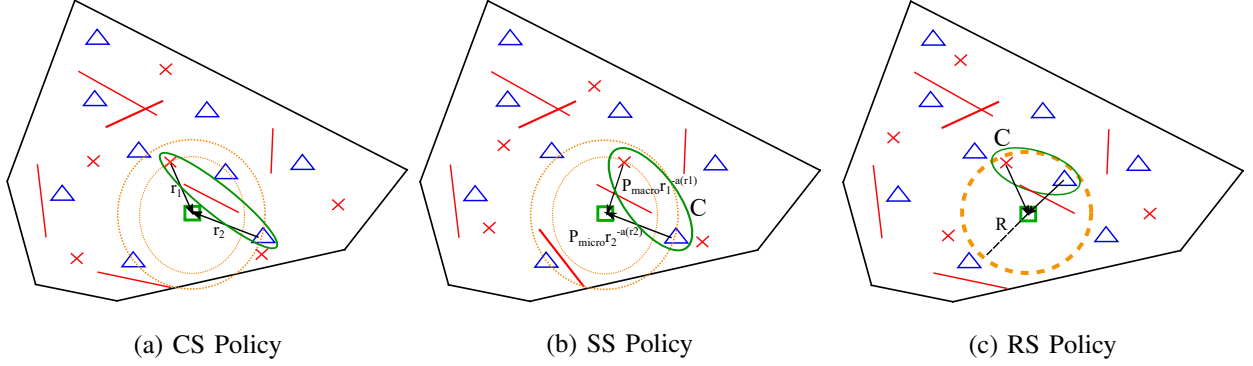


Fig. 1: The three considered pre-selection policies.

corresponds to a low implementation complexity. Therefore, it is appropriate for networks with strict power/bandwidth constraints. In this case, the set \mathcal{C}_{RS} is defined as

$$\mathcal{C}_{\text{RS}} = \{u_k^* : r_{u_k^*} \leq R, k \in \{1, \dots, K\}\}. \quad (6)$$

D. Implementation issues

In this subsection, we discuss the potential implementation of the proposed two-level BS selection scheme. Towards this direction, we assume a centralized controller, which takes as input the signal strength of the links between BSs and users and implements the proposed two-level BS selection schemes. This centralized implementation is in line with the cloud radio access network (C-RAN) architecture in 5G mobile communication systems, where the BSs functionalities from physical layer to the higher layers are managed by a centralized logic (cloud) [34]. On the other hand, channel estimation in 5G communication systems exploits the time division duplex reciprocity and is performed in the uplink through orthogonal pilots signals. *It is worth noting that techniques for estimating the direction of arrival, such as the codebook-based beamforming protocol, the multiple signal classification (MUSIC) or the estimation of signal parameters via rotational invariance techniques [5, Ch. 3], are also used to estimate the beamforming gain.* Therefore, the required information (i.e., strength of the links, beamforming gain) is obtained by using the pilot signals. This information is collected and measured by the BSs (i.e., remote radio heads in C-RAN) and is communicated to centralized unit through a fronthaul network.

IV. PERFORMANCE ANALYSIS

In this section, we analyze the SINR distribution for the downlink of a mmWave heterogeneous cellular network, where the terminals employ sectorized antennas in the presence of blockages.

We first characterize the overall SINR complimentary cumulative distribution function (CCDF) by analyzing the network when the desired link is either LOS and NLOS and finally we quantify the effect of random distances. Without loss of generality and following Slivnyak's theorem [33], we execute the analysis for a typical user located at the origin but the results hold for all users of the network. Using the proposed low-complexity two-level BS selection (BSS) technique, the network performance of each policy is derived analytically by using stochastic geometry.

Let SINR_k , represent the achieved instantaneous SINR when the user communicates with its pre-selected BS from the network tier k , written as

$$\text{SINR}_k = \frac{G_0 P_k r_{u_k^*}^{-a(r_{u_k^*})} h_{u_k^*}}{I + \sigma^2}, \quad (7)$$

where $I = \sum_{i=1}^K \sum_G \sum_{v_i \in \mathcal{Y}} G P_i h_{v_i} r_{v_i}^{-a(r_{v_i})}$ is the total received interfering power from all the active BSs in the network tier i where $\mathcal{Y} \subset \bigcup_{k=1}^K \Phi_k \setminus \mathcal{C}$; and $h_{u_k^*}$ is the channel fading between the user and its pre-selected BS, u_k^* , from the network tier k . By using the proposed technique, the controller selects the BS from the set of “candidate” BSs, that provides the maximum SINR i.e., $\text{SINR}^* \triangleq \max \{\text{SINR}_k\}$, where $k \in \{1, \dots, K\}$. The coverage probability $\mathcal{P}^*(T)$ at the user is the probability that the maximum SINR is greater than a predefined threshold T and is given by $\mathcal{P}^*(T) = \mathbb{P}[\text{SINR}^* \geq T]$. Therefore, with uncorrelated branches, the conditional density function (CDF) of SINR^* is

$$\mathbb{P}[\text{SINR}^* < T] = \prod_{k=1}^K \mathbb{P}[\text{SINR}_k < T] = \prod_{k=1}^K (1 - \mathcal{P}_k^*(T)), \quad (8)$$

where $\mathcal{P}_k^*(T)$ denotes the coverage probability of the user communicating with its pre-selected BS from network tier k . The link's status ℓ , between each user and its associated BS can be either LOS or NLOS. Hence, for a fixed distance $r_{u_k^*}$, between the user and its associated BS, we can use the law of total probability to expand the SINR CCDF as

$$\mathcal{P}_k^*(T \mid r_{u_k^*}) = \sum_{\ell \in \{\text{L}, \text{N}\}} \mathcal{P}_\ell \mathcal{P}_k^*(T \mid \ell, r_{u_k^*}), \quad (9)$$

where $\mathcal{P}_k^*(T \mid \ell, r_{u_k^*})$ is the achieved coverage probability of a user connecting with BS u_k^* from the tier k and with link status $\ell \in \{\text{L}, \text{N}\}$ and \mathcal{P}_ℓ expresses the probability that the link has status ℓ . By unconditioning on $r_{u_k^*}$, the achieved coverage probability from network tier k is written as

$$\mathcal{P}_k^*(T) = \int \cdots \int \sum_{\ell \in \{\text{L}, \text{N}\}} \mathcal{P}_\ell \mathcal{P}_k^*(T \mid \ell, r_{u_k^*}) f_\Phi^\Pi(\mathbf{r} \mid \ell) d\mathbf{r}, \quad (10)$$

where $f_{\Phi}^{\Pi}(\mathbf{r} \mid \ell)$ denotes the joint distribution of $\mathbf{r} = \{r_{u_1^*}, \dots, r_{u_K^*}\}$ for the pre-selection policy $\Pi \in \{\text{CS}, \text{SS}, \text{RS}\}$, given the status of the communication link is $\ell \in \{\text{L}, \text{N}\}$.

Based on the above, in the following subsections, we provide the coverage probability for each pre-selection policy.

A. CS policy

The CS policy pre-selects the closest LOS BSs from each tier of the network. Therefore, the following lemma provides the density of each tier together with the joint distance distribution when the CS policy is employed.

Lemma 1. *When the CS policy is employed, the density of the tier i is given by*

$$\lambda_i^{\text{CS}}(r \mid \text{L}) = 2\pi\lambda_i r \exp(-\beta r), \quad (11)$$

and the joint distance distribution between the user and its pre-selected BSs, is given by

$$f_{\Phi}^{\text{CS}}(\mathbf{r} \mid \text{L}) = \prod_{i=1}^K 2\pi\lambda_i r_{u_i^*} \exp\left(-\beta r_{u_i^*} - \frac{2\pi\lambda_i}{\beta^2} (1 - \exp(-\beta r_{u_i^*}) (1 + \beta r_{u_i^*}))\right). \quad (12)$$

Proof. See Appendix A. □

By using the above lemma, the following theorem provides the coverage probability achieved by the CS policy.

Theorem 1. *The coverage probability achieved when the CS policy is employed, is given by*

$$\mathcal{P}^*(T) < 1 - \prod_{k=1}^K \left(1 - \sum_{\xi=1}^{\nu_L} (-1)^{\xi+1} \binom{\nu_L}{\xi} \int \cdots \int_{0 < r_{u_1^*} < r_{u_2^*} < \cdots < \infty} \exp(-s_L \sigma^2) \mathcal{L}_I(s_L) f_{\Phi}^{\text{CS}}(\mathbf{r} \mid \text{L}) d\mathbf{r} \right), \quad (13)$$

where $f_{\Phi}^{\text{CS}}(\mathbf{r} \mid \text{L})$ is given by (12), and

$$\mathcal{L}_I(s_L) = \prod_{i=1}^K \prod_G \exp\left(-p_G \int_{r_{u_i^*}}^{\infty} \left(1 - \left(1 + \frac{s_L G P_i v^{-a_L}}{\nu_L}\right)^{-\nu_L}\right) \lambda_i^{\text{CS}}(v \mid \text{L}) dv\right), \quad (14)$$

where $G \in \{M^2, Mm, m^2\}$, $s_L = \frac{\eta_L \xi T r_{u_k^*}^{a_L}}{G_0 P_k}$, $\eta_L = \nu_L (\nu_L!)^{-1/\nu_L}$ and $\lambda_i^{\text{CS}}(v \mid \text{L})$ is given by (11).

Proof. See Appendix B. □

The above expression provides a general result for the coverage probability when the CS policy is applied. Even from this general expression, we can extract some observations towards its behavior. Initially, we can easily observe that by increasing the Nakagami parameter ν_L ,

the fading becomes less severe providing a better performance. Moreover, it is clear that by increasing the number of tiers, we can further boost the network performance due to the increase in diversity. In order to gain more insight into the network's performance, we make some additional assumptions in order to further simplify the above expression. Firstly, we assume that the interfering links do not experience any fading. This assumption is based on the fact that small-scale fading has a relatively minor impact in mmWave cellular networks [4]. Also, based on the nature of a mmWave signal, we assume a highly directional beam pattern with high main-lobe gain i.e., $M \rightarrow \infty$. Finally, we consider the case of an ultra-dense deployment of the BSs. We consider the two extreme cases that provide the bounds of the network performance: *i*) Lower bound: all BSs are in NLOS with the user ($\beta \rightarrow \infty$) and *ii*) Upper bound: all BSs are in LOS with the user ($\beta \rightarrow 0$). Then, from these assumptions, we can state the following.

Remark 1. *In an ultra-dense network, the coverage probability for the CS policy is given by*

$$\mathcal{P}^*(T) < 1 - \prod_{k=1}^K \left(1 - \sum_{\xi=1}^{\nu_\ell} \frac{(-1)^{\xi+1} \binom{\nu_\ell}{\xi}}{1 + \eta_\ell \xi T \frac{m^2}{G_0} \Gamma \left[1 - \frac{2}{a_\ell} \right] \frac{\sum_{i=1}^K \lambda_i P_i^{\frac{2}{a_\ell}}}{\lambda_k P_k}} \right), \quad (15)$$

where $\ell = N$ for $\beta \rightarrow \infty$, $\ell = L$ for $\beta \rightarrow 0$ and $\eta_\ell = \nu_\ell (\nu_\ell!)^{-1/\nu_\ell}$.

Proof. See Appendix C. □

From (15) we can easily obtain the same observations as before regarding the number of tiers and the Nakagami parameter. However, from this simplified expression, we can also deduce that the achieved coverage performance increases with the transmit power of BSs P_k , $k \in \{1, \dots, K\}$ until a certain point. By further increasing the transmit power, the ratio $\frac{\sum_{i=1}^K P_i^{2/a_L}}{P_k} \rightarrow 1$, thus the network performance converges to a constant floor. This observation is due to the increasing interfering power faced by the user which equalizes the desired received signal.

B. SS policy

We now consider the case where the SS policy is employed. Let $\Psi_k = \left\{ r_{u_k^*}^{a(r_{u_k^*})} / P_k, u_k^* \in \Phi_k \right\}$, $k \in \{1, \dots, K\}$, denote the normalized path-loss between each BS in Φ_k and its associated user and let $\gamma_k = r_{u_k^*}^{a(r_{u_k^*})} / P_k$ be the elements of Ψ_k . The normalized path-loss between the user and its pre-selected BS from tier k is given by γ_k^* . Let $\gamma = (\gamma_1^*, \dots, \gamma_K^*)$, then by the mapping theorem [33], Ψ_k is a PPP with density $\lambda_k(\gamma)$ and joint distribution $f_\Psi(\gamma)$ which are given in the following lemma.

Lemma 2. When the SS policy is employed, the density of the tier i is given by

$$\lambda_i^{\text{SS}}(\gamma \mid \text{L}) = \frac{2\pi\lambda_i}{a_L} P_i^{\frac{2}{a_L}} \gamma^{\frac{2}{a_L}-1} \exp\left(-\beta(P_i\gamma)^{\frac{1}{a_L}}\right) \text{ and} \quad (16)$$

$$\lambda_i^{\text{SS}}(\gamma \mid \text{N}) = \frac{2\pi\lambda_i}{a_N} P_i^{\frac{2}{a_N}} \gamma^{\frac{2}{a_N}-1} \left(1 - \exp\left(-\beta(P_i\gamma)^{\frac{1}{a_N}}\right)\right), \quad (17)$$

and the joint distance distributions between the user and its pre-selected BSs are given by

$$\begin{aligned} f_{\Psi}^{\text{SS}}(\gamma \mid \text{L}) &= \prod_{i=1}^K \frac{2\pi\lambda_i}{a_L} P_i^{\frac{2}{a_L}} (\gamma_i^*)^{\frac{2}{a_L}-1} \exp\left(-\beta(P_i\gamma_i^*)^{\frac{1}{a_L}}\right) \\ &\times \exp\left(-\frac{2\pi\lambda_i}{\beta^2} \left(1 - \exp\left(-\beta(P_i\gamma_i^*)^{\frac{1}{a_L}}\right) \left(1 + \beta(P_i\gamma_i^*)^{\frac{1}{a_L}}\right)\right)\right), \end{aligned} \quad (18)$$

$$\begin{aligned} f_{\Psi}^{\text{SS}}(\gamma \mid \text{N}) &= \prod_{i=1}^K \frac{2\pi\lambda_i}{a_N} P_i^{\frac{2}{a_N}} (\gamma_i^*)^{\frac{2}{a_N}-1} \left(1 - \exp\left(-\beta(P_i\gamma_i^*)^{\frac{1}{a_N}}\right)\right) \\ &\times \exp\left(-\pi\lambda_i(P_i\gamma_i^*)^{\frac{1}{a_N}} - \frac{2\pi\lambda_i}{\beta^2} \left(1 - \exp\left(-\beta(P_i\gamma_i^*)^{\frac{1}{a_N}}\right) \left(1 + \beta(P_i\gamma_i^*)^{\frac{1}{a_N}}\right)\right)\right). \end{aligned} \quad (19)$$

Proof. See Appendix D. \square

Following a similar methodology as for the CS policy, the Laplace transform for the interference I_i of the BSs that belong in network tier i , can be written as

$$\mathcal{L}_{I_i}(s \mid G, \ell) = \exp\left(-p_G \int_{\gamma_i^*}^{\infty} (1 - \mathbb{E}_h[\exp(-s_{\ell} G h v^{-1})]) \lambda_i^{\text{SS}}(v \mid \ell) dv\right), \quad (20)$$

where $s_{\ell} = \frac{\eta_{\ell} \xi^T \gamma_k^*}{G_0}$, $\eta_{\ell} = \nu_{\ell}(\nu_{\ell}!)^{-1/\nu_{\ell}}$ and $\lambda_i^{\text{SS}}(v \mid \ell)$ denotes the density of the BSs of which the link with the user has status $\ell \in \{\text{L}, \text{N}\}$. Now, using the moment-generating function (MGF) of the Gamma random variable h as before, the above expression is given by

$$\mathcal{L}_{I_i}(s \mid G, \ell) = \exp\left(-p_G \int_{\gamma_i^*}^{\infty} \left(1 - \left(1 + \frac{s_{\ell} G v^{-1}}{\nu_{\ell}}\right)^{-\nu_{\ell}}\right) \lambda_i^{\text{SS}}(v \mid \ell) dv\right). \quad (21)$$

We can now state the following theorem which provides an the coverage probability achieved by the SS policy.

Theorem 2. The coverage probability achieved when the SS policy is employed, is given by

$$\begin{aligned} \mathcal{P}^*(T) &< 1 - \prod_{k=1}^K \left(1 - \sum_{\xi=1}^{\nu_L} (-1)^{\xi+1} \binom{\nu_L}{\xi} \int_{0 < \gamma_1^* < \gamma_2^* < \dots < \infty} \exp(-s_L \sigma^2) \mathcal{L}_I(s_L) f_{\Psi}^{\text{SS}}(\gamma \mid \text{L}) d\gamma \right. \\ &\quad \left. - \sum_{\xi=1}^{\nu_N} (-1)^{\xi+1} \binom{\nu_N}{\xi} \int_{0 < \gamma_1^* < \gamma_2^* < \dots < \infty} \exp(-s_N \sigma^2) \mathcal{L}_I(s_N) f_{\Psi}^{\text{SS}}(\gamma \mid \text{N}) d\gamma \right), \end{aligned} \quad (22)$$

where $f_{\Psi}^{\text{SS}}(\gamma \mid \text{L})$ and $f_{\Psi}^{\text{SS}}(\gamma \mid \text{N})$ are given by (18) and (19), respectively,

$$\mathcal{L}_I(s_{\text{L}}) = \prod_{i=1}^K \prod_{\ell} \prod_G \exp \left(-p_G \int_{\gamma_i^*}^{\infty} \left(1 - \left(1 + \frac{s_L G v^{-1}}{\nu_{\ell}} \right)^{-\nu_{\ell}} \right) \lambda_i^{\text{SS}}(v \mid \ell) dv \right), \quad (23)$$

and

$$\mathcal{L}_I(s_{\text{N}}) = \prod_{i=1}^K \prod_{\ell} \prod_G \exp \left(-p_G \int_{\gamma_i^*}^{\infty} \left(1 - \left(1 + \frac{s_N G v^{-1}}{\nu_{\ell}} \right)^{-\nu_{\ell}} \right) \lambda_i^{\text{SS}}(v \mid \ell) dv \right), \quad (24)$$

where $G \in \{M^2, Mm, m^2\}$, $\ell \in \{L, N\}$, $s_{\ell} = \frac{\eta_{\ell} \xi T \gamma_k^*}{G_0}$, $\eta_{\ell} = \nu_{\ell}(\nu_{\ell}!)^{-1/\nu_{\ell}}$ and $\lambda_i^{\text{SS}}(v \mid \ell)$ is given by Lemma 2.

Proof. The proof follows similar methodology as described in Appendix B, but using the Laplace transform of interference function obtained by the multiplication of the associated sub-PPPs that are given by the expression in (21). \square

The expression in (22) provides a general result for the coverage probability when the SS policy is applied. Even from this general expression, we can extract some observations towards its behavior. We can easily observe the positive impact of the number of network tiers and the Nakagami parameter on the network's coverage probability. In order to gain more insight into the network's performance, we make similar assumptions as with the case of CS policy in order to further simplify the above expression. We consider the two extreme cases that provide the bounds of the network performance: *i)* Lower bound: all BSs are in NLOS with the user ($\beta \rightarrow \infty$) and *ii)* Upper bound: all BSs are in LOS with the user ($\beta \rightarrow 0$). Then, from these assumptions, we can state the following.

Remark 2. In an ultra-dense network, the coverage probability for the SS policy is given by

$$\mathcal{P}^*(T) < 1 - \prod_{k=1}^K \left(1 - \sum_{\xi=1}^{\nu_{\ell}} (-1)^{\xi+1} \binom{\nu_{\ell}}{\xi} \int_0^{\infty} \dots \int_0^{\infty} \prod_{k=1}^K \exp \left(-\pi \lambda_i \left(\frac{\eta_{\ell} \xi T P_i m^2}{\gamma_i^* G_0} \right)^{\frac{2}{a_{\ell}}} \Gamma \left[1 - \frac{2}{a_{\ell}} \right] \right) f_{\Psi}^{\text{SS}}(\gamma \mid \ell) d\gamma \right), \quad (25)$$

where $\ell = N$ for $\beta \rightarrow \infty$, $\ell = L$ for $\beta \rightarrow 0$ and $\eta_{\ell} = \nu_{\ell}(\nu_{\ell}!)^{-1/\nu_{\ell}}$.

Proof. The proof follows similar steps as in Appendix C. \square

From (25), we can easily the same observations as before regarding the number of tiers and the Nakagami parameter. However, from this simplified expression, we can also deduce that the coverage threshold is inversely proportional to the network performance.

Aiming to measure the reliability of the wireless communication scheme under fading, we study the achieved diversity by employing the SS policy. The standard definition of the diversity is based on the high SINR analysis. For the special case where the Nakagami- m parameters for both LOS and NLOS communication links are assumed equal to $\nu_L = \nu_N = 1$, in the following Remark we derive the diversity order by considering the SS pre-selection policy for the special case where Rayleigh fading is adopted.

Remark 3 (Diversity Gain). The numerator of (7) is an independent exponentially distributed random variable with probability density function $\xi_k \exp(-\xi_k x)$, $x \geq 0$ with $\xi_k = \frac{1}{G_0 \gamma_k^*}$. By letting $I' = I + \sigma^2$, the outage probability is given by

$$\begin{aligned} \mathbb{P}[\text{SINR}^* < T] &= \prod_{k=1}^K \mathbb{P}[\text{SINR}_k < T] = \prod_{k=1}^K \mathbb{P}[G_0 \gamma_k^* h_{\gamma_k^*} < T I'] \\ &= \prod_{k=1}^K \mathbb{E}_{\gamma_k^*, I'} \left[\int_0^{T I'} \xi_k \exp(-\xi_k x) dx \right] = T^K \prod_{k=1}^K \mathbb{E}_{\gamma_k^*, I'} \left[I' \int_0^1 \xi_k \exp(-\xi_k T I' z) dz \right], \end{aligned} \quad (26)$$

which follows from the change of variable $x = T I' z$. At the high coverage regime i.e., $T \rightarrow 0$, we have

$$I' \int_0^1 \xi_k \exp(-\xi_k T I' z) dz \sim I' \int_0^1 \xi_k dz.$$

As a result,

$$\mathbb{P}[\text{SINR}^* < T] \approx T^K \prod_{k=1}^K \mathbb{E}_{\gamma_k^*, I'} [I' \xi_k]. \quad (27)$$

By substituting the expression (27) into the expression for diversity order of interference-limited networks, we have

$$\lim_{T \rightarrow 0} \frac{\log(1 - \mathcal{P}^*(T))}{\log(T)} = \lim_{T \rightarrow 0} \left(\frac{\log T^K}{\log T} + \frac{\log \left(\prod_{k=1}^K \mathbb{E}_{\gamma_k^*, I'} [I' \xi_k] \right)}{\log T} \right) = K, \quad (28)$$

due to the fact that the second term of the equation for $T \rightarrow 0$ converges to zero. As a result, the diversity order of the proposed scheme when the user employs the SS policy, is equal to K .

C. RS policy

The RS scheme randomly pre-selects a BS among the ones located within a disk of radius R around the user. The user is in outage when the disk is empty or when the selected BS cannot

support the target SINR threshold. By considering these events, the coverage probability is given by the following theorem.

Lemma 3. *When the RS policy is employed, the density of the tier i is given by*

$$\lambda_i^{\text{RS}}(r \mid \text{L}) = 2\pi\lambda_i r \exp(-\beta r) \quad \text{and} \quad \lambda_i^{\text{RS}}(r \mid \text{N}) = 2\pi\lambda_i r (1 - \exp(-\beta r)), \quad r \leq R,$$

and the joint distance distributions between the user and its pre-selected BSs, are given by

$$f_{\Phi}^{\text{RS}}(\mathbf{r} \mid \text{L}) = \left(\frac{2}{R^2}\right)^K \prod_{i=1}^K r_{u_i^*} \exp(-\beta r_{u_i^*}), \quad (29)$$

$$f_{\Phi}^{\text{RS}}(\mathbf{r} \mid \text{N}) = \left(\frac{2}{R^2}\right)^K \prod_{i=1}^K r_{u_i^*} (1 - \exp(-\beta r_{u_i^*})). \quad (30)$$

Proof. The BSs that belong in the disk of radius R around the user, are uniformly distributed, thus creating a Matern cluster process [35]. The density function of those points is given by $f(r) = \frac{2r}{R^2}$ and the result follows. \square

Theorem 3. *The coverage probability achieved when the RS policy is employed, is given by*

$$\begin{aligned} \mathcal{P}^*(T) &< 1 - \prod_{k=1}^K \left(\exp(-\lambda_k \pi R^2) + (1 - \exp(-\lambda_k \pi R^2)) \left(1 \right. \right. \\ &\quad \left. \left. - \sum_{\xi=1}^{\nu_L} (-1)^{\xi+1} \binom{\nu_L}{\xi} \int \cdots \int_{0 < r_{u_1^*} < r_{u_2^*} < \cdots < \infty} \exp(-s_L \sigma^2) \mathcal{L}_I(s_L) f_{\Phi}^{\text{RS}}(\mathbf{r} \mid \text{L}) d\mathbf{r} \right. \right. \\ &\quad \left. \left. - \sum_{\xi=1}^{\nu_N} (-1)^{\xi+1} \binom{\nu_N}{\xi} \int \cdots \int_{0 < r_{u_1^*} < r_{u_2^*} < \cdots < \infty} \exp(-s_N \sigma^2) \mathcal{L}_I(s_N) f_{\Phi}^{\text{RS}}(\mathbf{r} \mid \text{N}) d\mathbf{r} \right) \right), \end{aligned} \quad (31)$$

where $f_{\Phi}^{\text{RS}}(\mathbf{r} \mid \text{L})$ and $f_{\Phi}^{\text{RS}}(\mathbf{r} \mid \text{N})$ are given by (29) and (30), respectively,

$$\mathcal{L}_I(s_L) = \prod_{i=1}^K \prod_{\ell} \prod_G \exp \left(-p_G \int_{r_{u_k^*}}^{\infty} \left(1 - \left(1 + \frac{s_L G P_i v^{-a_L}}{\nu_{\ell}} \right)^{-\nu_{\ell}} \right) \lambda_i^{\text{RS}}(v \mid \ell) dv \right), \quad (32)$$

and

$$\mathcal{L}_I(s_N) = \prod_{i=1}^K \prod_{\ell} \prod_G \exp \left(- \int_{r_{u_k^*}}^{\infty} \left(1 - \left(1 + \frac{s_N G P_i v^{-a_N}}{\nu_{\ell}} \right)^{-\nu_{\ell}} \right) \lambda_i^{\text{RS}}(v \mid \ell) dv \right), \quad (33)$$

where $G \in \{M^2, Mm, m^2\}$, $s_{\ell} = \frac{\eta_{\ell} \xi T \gamma_k^*}{G_0}$, $\ell \in \{L, N\}$, $\eta_{\ell} = \nu_{\ell}(\nu_{\ell}!)^{-1/\nu_{\ell}}$ and $\lambda_i^{\text{RS}}(v \mid \ell)$ is given by Lemma 3.

Proof. The proof follows the same methodology as described in Appendix B, but with the density and joint distribution functions that correspond to the RS policy. Furthermore, the case where the disk of radius R is empty needs to be consider, so the probability of this event occurring is given by $\exp(-\lambda_k \pi R^2)$ [33]. \square

V. SUCCESSIVE INTERFERENCE CANCELLATION

In this section, we discuss the additional achieved gains on the network performance, by exploiting the ability of the users to perform SIC. Even though SIC is characterized by high computational demand, its application is considered as a special case aiming for the further boost of the network performance. In order to maintain the complexity at a lower level, we assume that the small-scale fading between the user and its associated BS is modeled as Rayleigh fading. Thus, we assume that the Nakagami- m parameters for LOS and NLOS communication links fulfill the expression $\nu_L = \nu_N = 1$. The main idea of SIC is to decode the dominant interference signals and subtract them from the received signal, resulting in an increase of the observed SINR. We assume that each user has the ability to implement an ideal SIC in accordance to [32]. The number of interferers that can be canceled is assumed to be limited to $N \in \mathbb{N}$ in order to keep both the computational complexity and power consumption at low levels.

At the beginning, the user attempts to decode the received signal without any interference cancellation. If this attempt is unsuccessful, the user seeks to decode the dominant interfering signal, subtract it from the received signal, and then re-attempt to decode the resulting received signal. We assume that the order statistics of the received interfering signal power do not depend on the fading and are determined by the distances [29]. The received signal power at the user can be ordered as $\{X_{(1)}, X_{(2)}, \dots\}$ such that $X_{(i)} \geq X_{(j)}$, with $i \leq j$ where $X_{(j)}$ represent the received signal from the j -th strongest interfering BS. The previous actions are repeated up to N times until the received signal is decoded, while satisfying the constraint on the maximum number of cancellations; otherwise, the user is considered to be in outage. Hence, the transmission is successful as long as one of the following events is successful

$$\begin{aligned}
 &0 : (\text{SINR}(0) \geq T) \\
 &1 : (\text{SINR}(0) < T) \cap \left(\frac{X_{(1)}}{I^{(1)} + \sigma^2} \geq T \right) \cap (\text{SINR}(1) \geq T) \\
 &\vdots \\
 &N : \left(\bigcap_{n=0}^{N-1} \text{SINR}(n) < T \right) \cap \left(\bigcap_{n=1}^N \frac{X_{(n)}}{I^{(n)} + \sigma^2} \geq T \right) \cap (\text{SINR}(N) \geq T), \quad (34)
 \end{aligned}$$

where $\text{SINR}(n)$ represents the observed SINR from the user after the cancelation of the n -th strongest interfering signals and $I^{(n)}$ represents the aggregate interference after the cancellation of the n -th strongest interfering BSs.

The first term in (34) represents the outage probability for decoding the received signal, when the user cancels $n-1$ interferers, while the third term denotes the success probability of decoding the received signal after n successful cancellations. Finally, the second term of (34) represents the event of successfully canceling the n -th interferer.

For the study of the Laplace transform of the partially canceled interference depending on the pre-selection policy, we state the following Lemma.

Lemma 4. *The Laplace transform of the partially cancelled interference function $I^{(n)}$ is given by*

$$\mathcal{L}_{I^{(n)}}^{\text{CS}}(s_L) = \prod_{i=1}^K \prod_G \exp \left(-p_G \int_{R^*(n,k)}^{\infty} \frac{s_L G P_i v^{-a_L}}{1 + s_L G P_i v^{-a_L}} \lambda_i^{\text{CS}}(v | L) dv \right), \quad (35)$$

for the CS policy,

$$\mathcal{L}_{I^{(n)}}^{\text{SS}}(s) = \prod_{i=1}^K \prod_{\ell} \prod_G \exp \left(-p_G \int_{V^*(n,k)}^{\infty} \frac{s G v^{-1}}{1 + s G v^{-1}} \lambda_i^{\text{SS}}(v | \ell) dv \right), \quad (36)$$

for the SS policy,

$$\mathcal{L}_{I^{(n)}}^{\text{RS}}(s) = \prod_{i=1}^K \prod_{\ell} \prod_G \exp \left(-p_G \int_0^{\infty} \frac{s G P_i v^{-a_{\ell}}}{1 + s G P_i v^{-a_{\ell}}} \lambda_i^{\text{RS}}(v | \ell) dv \right), \quad (37)$$

for the RS policy, where $G \in \{M^2, Mm, m^2\}$, $s = \{s_L, s_N\} = \left\{ \frac{\eta_L \xi^T \gamma_k^*}{G_0}, \frac{\eta_N \xi^T \gamma_k^*}{G_0} \right\}$ takes values depending on whether the direct link is LOS and NLOS, respectively; $R^*(n, k) = \sqrt{\frac{n}{\lambda_k \pi}}$ represents the cancellation radius of the interference-free area around the user, which successfully canceled n interfering BSs from network tier k and $V^*(n, k) = \frac{R^*(n, k)^{a(r_{u_k^*})}}{P_k}$ represents the normalised path loss of the cancellation radius.

Proof. The proof follows similar steps as in Appendix B, where in this case, we have different regions in which the interfering BSs exist. Specifically, the observed interference originates from BSs which are located outside the interference-free area around the user with cancellation radius $R^*(n, k)$. Hence, the lower limit of the integral of the Laplace transform is defined by the cancellation radius of the user. \square

Firstly, we define the probability of successfully decoding the desired signal by the user, after cancelling the n interferers. Given that n interferers have been canceled, the instantaneous coverage probability of the network tier k can be defined as in the following Lemma.

Lemma 5. *Given that n strongest interferers have been canceled, the successful coverage performance, is given by*

$$\mathcal{P}_S(n, T) = 1 - \prod_{k=1}^K \left(1 - \int_{0 < r_{u_1^*} < r_{u_2^*} < \dots < \infty} \exp(-s\sigma^2) \mathcal{L}_{I^{(n)}}^\Pi(s_L) f_\Phi^\Pi(\mathbf{r} \mid L) d\mathbf{r} \right. \\ \left. - \int_{0 < r_{u_1^*} < r_{u_2^*} < \dots < \infty} \exp(-s\sigma^2) \mathcal{L}_{I^{(n)}}^\Pi(s_N) f_\Phi^\Pi(\mathbf{r} \mid N) d\mathbf{r} \right), \quad (38)$$

where $f_\Phi^\Pi(\mathbf{r} \mid \ell)$ is analysed in Section III and it depends on the pre-selection policy $\Pi \in \{CS, SS, RS\}$ and the link status $\ell \in \{L, N\}$, $s_L = \frac{\eta_L \xi T \gamma_k^*}{G_0}$, $s_N = \frac{\eta_N \xi T \gamma_k^*}{G_0}$ and the expressions of $\mathcal{L}_{I^{(n)}}^\Pi(s_L)$ and $\mathcal{L}_{I^{(n)}}^\Pi(s_N)$ are given by Lemma 4 depending on the adopted pre-selection policy.

Proof. We define the instantaneous success probability for the network tier k after successfully canceling n interferers as

$$\mathcal{P}_S(n, k, T) = \mathbb{P} [\text{SINR}_k(n) > T (I^{(n)} + \sigma^2)] = \mathbb{P} \left[P_k G_{u_k^*} h_{u_k^*} r_{u_k^*}^{-a(r_{u_k^*}^*)} > T (I^{(n)} + \sigma^2) \right] \\ = \mathbb{P} \left[h_{u_k^*} > \frac{T r_{u_k^*}^{a(r_{u_k^*}^*)}}{P_k G_{u_k^*}} (I^{(n)} + \sigma^2) \right] = \mathbb{E}_{\mathbf{r}} [\mathcal{L}_{I^{(n)}}(s) \exp(-s\sigma^2)], \quad (39)$$

which follows from the fact that $h_{u_k^*}$ is an exponentially distributed random variable, hence $P_k G_{u_k^*} h_{u_k^*} r_{u_k^*}^{-a(r_{u_k^*}^*)}$ is exponentially distributed with mean $P_k G_{u_k^*} r_{u_k^*}^{-a(r_{u_k^*}^*)}$; (39) follows with the use of the Laplace transform of $I^{(n)}$ that takes values according to Lemma 4. To find the unconditional success probability, we take the expectation over r_k^* and by using the proposed BSS technique, we conclude to (38). \square

In the following discussion, we derive the success probability of the user to decode and cancel the n -th strongest interferer, with the assumption that the interference for the $n - 1$ strongest interfering BSs has been previously canceled.

Lemma 6. *The coverage probability of a user attempting to decode the n -th strongest interfering signal, is given by*

$$\mathcal{P}_S(n, T) = 1 - \prod_{k=1}^K \left(1 - \int_{0 < r_{u_1^*} < r_{u_2^*} < \dots < \infty} \exp(-s\sigma^2) \mathcal{L}_{I^{(n)}}^\Pi(s_L) f_\Phi(\mathbf{r}, n \mid L) d\mathbf{r} \right. \\ \left. - \int_{0 < r_{u_1^*} < r_{u_2^*} < \dots < \infty} \exp(-s\sigma^2) \mathcal{L}_{I^{(n)}}^\Pi(s_N) f_\Phi(\mathbf{r}, n \mid N) d\mathbf{r} \right), \quad (40)$$

where $s_L = \frac{\eta_L \xi T \gamma_k^*}{G_0}$, $s_N = \frac{\eta_N \xi T \gamma_k^*}{G_0}$; the expressions of $\mathcal{L}_{I^{(n)}}^\Pi(s_L)$ and $\mathcal{L}_{I^{(n)}}^\Pi(s_N)$ are given by Lemma 4 depending on the adopted pre-selection policy and $f_\Phi(\mathbf{r}, n \mid L)$ and $f_\Phi(\mathbf{r}, n \mid N)$ denote the joint distance distribution between the user and the n -th nearest LOS and NLOS BS from each network tier i , respectively, and is given by

$$f_\Phi(\mathbf{r}, n \mid L) = \prod_{i=1}^K \exp(-\Lambda_i(r_n \mid L)) \frac{\Lambda_i(r_n \mid L)^n}{n!} \quad f_\Phi(\mathbf{r}, n \mid N) = \prod_{i=1}^K \exp(-\Lambda_i(r_n \mid N)) \frac{\Lambda_i(r_n \mid N)^n}{n!}, \quad (41)$$

where $\Lambda_i(r_n \mid L)$ and $\Lambda_i(r_n \mid N)$ represent the intensity measure of LOS and NLOS BSs in network tier i , respectively.

Proof. After successfully decoding and subtracting $n - 1$ signals from the received signal, the probability of successfully decoding the n -th interfering BS from network tier k , conditioned on its distance, r_n , can be written as

$$\mathcal{P}_D(n, k, T \mid r_n) = \mathbb{P} \left[h_{r_n} > \frac{T(I^{(n)} + \sigma^2)}{G_0 P_k r_n^{-a(r_n)}} \right] = \exp(-s\sigma^2) \mathcal{L}_{I^{(n)}}^\Pi(s), \quad (42)$$

where $s = \{s_L, s_N\} = \left\{ \frac{\eta_L \xi T \gamma_k^*}{G_0}, \frac{\eta_N \xi T \gamma_k^*}{G_0} \right\}$ takes value depending on whether the direct link is LOS and NLOS, respectively and the value of $\mathcal{L}_{I^{(n)}}^\Pi(s)$ is given based on Lemma 4. To find the unconditional success probability, the expectation should be taken with respect to the distance of the n -th interferer with PDF that is given by expression (41). Based on the density expressions for each pre-selection policy that are analyzed in Section III, the intensity measure is equal to $\Lambda_i(r_n) = \int_0^{r_n} \lambda_i(u) du$. By using the proposed BSS scheme, we conclude to (40). \square

Note that when $N = 0$ i.e., no interferers have been cancelled, the achieved coverage performance with the use of the SIC scheme $\mathcal{P}_{\text{SIC}}(T, N)$ is equal to the coverage probability when no SIC is applied, that is $\mathcal{P}_{\text{SIC}}(T, 0) = \mathcal{P}^*(T)$. We now provide the coverage performance of a receiver with SIC capabilities. Based on the sequence of events in (34), the following theorem provides the overall coverage performance.

Theorem 4. *The coverage performance \mathcal{P}_{SIC} for a downlink user with the ability to perform SIC to cancel a maximum of N interferers, is given by,*

$$\mathcal{P}_{\text{SIC}}(T, N) = \mathcal{P}^*(T) + \sum_{z=1}^N \left(\prod_{n=0}^{z-1} (1 - \mathcal{P}_S(n, T)) \right) \left(\prod_{n=1}^z \mathcal{P}_D(n, T) \right) \mathcal{P}_S(z, T). \quad (43)$$

Proof. Since the success of SIC occurs as one of the steps described in (34), the proof follows directly from the definition of the sequence of events and the derivation of $\mathcal{P}_S(n, T)$ and $\mathcal{P}_D(n, T)$. \square

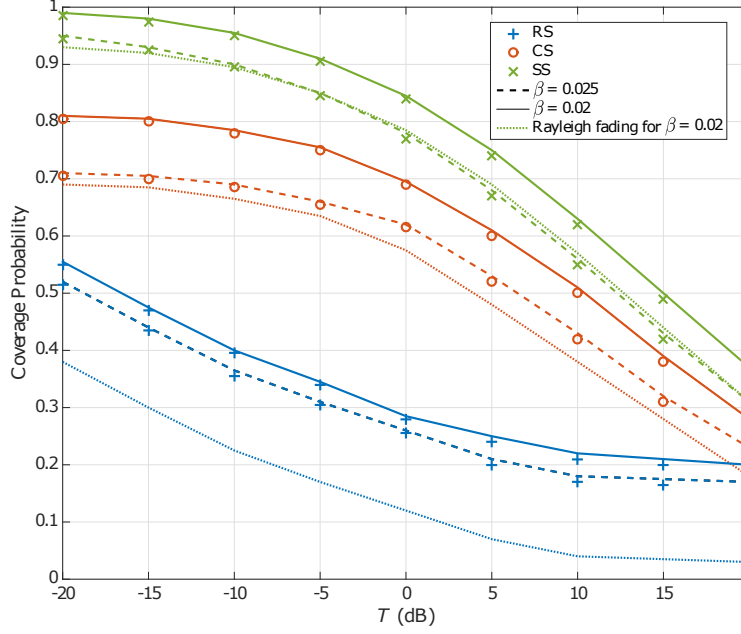


Fig. 2: Coverage probability versus the threshold T for different values of blockage constant $\beta = \{0.02, 0.025\}$; the lines and markers represent the theoretical and simulation results, respectively.

VI. NUMERICAL RESULTS

In this section, we provide numerical results to verify our model and illustrate the effectiveness and potential benefits of the proposed BSS scheme. We focus on the special case of a heterogeneous network with $K = 2$ tiers i.e., consisting of a macro-tier overlaid with a pico-tier. We assume that the BS density of the first and second tier is $\lambda_1 = 5 \times 10^{-5}$ and $\lambda_2 = 3\lambda_1$, respectively; the transmit power for each network tier is $P_1 = 40$ dB and $P_2 = 20$ dB, respectively. Furthermore, we assume that the non-negative blockage constant is $\beta = 0.02$. The noise power is set to $\sigma^2 = -70$ dB. The Nakagami fading parameters for LOS and NLOS links are set to $\nu_L = 4$ and $\nu_N = 2$, while the path loss exponents are set to $a_L = 2$ and $a_N = 4$, respectively. The parameters for the sectorized antenna model are set to $M = 10$ for the main lobe gain, $m = 0.1$ for side lobe gain and $\theta = \frac{\pi}{6}$ for the main lobe beamwidth [23].

Fig. 2 illustrates the effects of blockage/obstacles on the network performance for the proposed pre-selection policies. We can first observe that the analytical results provide an upper bound for the network performance given by the simulation results; this is expected due to Alzer's Lemma [36]. Furthermore, it is clear from the figure, that with the increase of blockage density there is a significant loss in coverage performance. This again is expected, since by increasing the blockage density, more and more links between the users and their associated BSs are in NLOS.

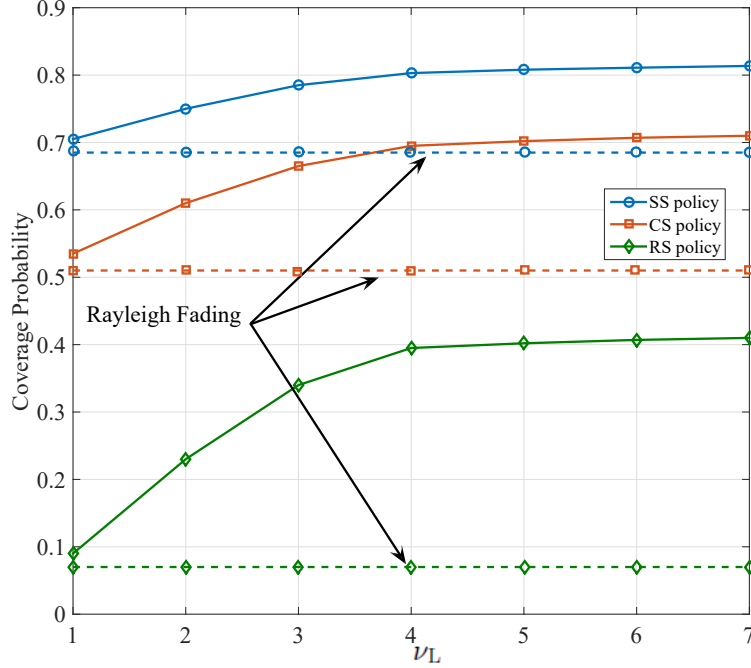


Fig. 3: Coverage probability versus the Nakagami parameter ν_N for the pre-selection policies; $\nu_L = 2\nu_N$, $T = 5$ dB.

Therefore, the probability that the user connects to a LOS BS is decreased so the signal at the user becomes weaker and the received SINR is reduced. Another important observation from this figure is that the SS policy achieves a significantly higher network performance, outperforming the other two policies.

In Fig. 3, the network coverage performance over Nakagami fading is plotted for all the pre-selection policies. For comparison reasons, the network performance over Rayleigh fading for each pre-selection policy is also displayed in the figure as a dashed line. Based on the figure, we observe that the increase of the Nakagami parameter ν results in an increase of the coverage probability in all pre-selection policies. This observation can be explained by the fact that by increasing the quality of the communication link, users experience lower fading over their received signal, thus the network performance increase. Furthermore, it can be easily seen that, as $\nu_\ell \rightarrow \infty$, the network performance becomes independent of the Nakagami parameter. This was expected due to the fact that, while $\nu_\ell \rightarrow \infty$, the fading becomes a deterministic value centered on the mean. Finally, by comparing the achieved network performance between the cases of Nakagami and Rayleigh fading, we noticed that for low Nakagami parameters, the analysis of network performance with the latter case provides a lower bound of the first case.

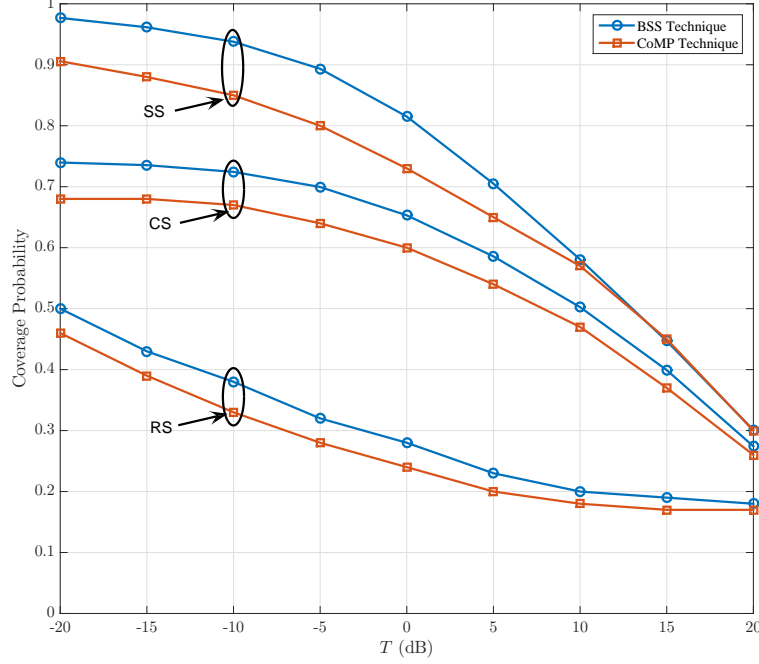


Fig. 4: Coverage probability versus the threshold T for the BSS and CoMP schemes; $\beta = 0.025$.

For this reason and for the rest of this paper, we continue our analysis on the assumption that the attenuation between users and BSs is a Rayleigh fading.

Fig. 4 shows the network coverage performance of the proposed BSS technique compared to the conventional coordinated multipoint (CoMP) technique for each pre-selection policy [11]. CoMP technique allows multiple randomly distributed BSs to jointly transmit data to a user. On the other hand, by using BSS technique, each user is able to communicate with the BS that provides the maximum SINR and which belongs in the set of “candidate” BSs. Hence, in order to conduct a fair comparison between the CoMP technique and the BSS technique, we assume that the transmit power of the terminals that belong in the network tier k and employ CoMP technique, is equal to $P_k^{\text{CoMP}} = P_k/K$; this assumption ensures the same total transmit power of both techniques. As it can be seen, our proposed technique offers marginal coverage performance gains when compared to the CoMP technique with lower computational demands. Particularly, the selection of a single BS for the communication, opposed to the joint transmission of multiple BSs, reduces the existing interference and thus the network performance is increased.

Fig. 5 shows the impact of cooperation on the achieved coverage performance with respect to the BSs’ transmit power for $K = \{1, 2, 3\}$. For the cases $K = 2$ and $K = 3$, we assume that the transmit power of the BSs in each tier is inversely proportional to the tier’s density. Specifically, we assume $\lambda_1 < \lambda_2 < \lambda_3$ and so $P_1 > P_2 > P_3$. The first main observation is that as

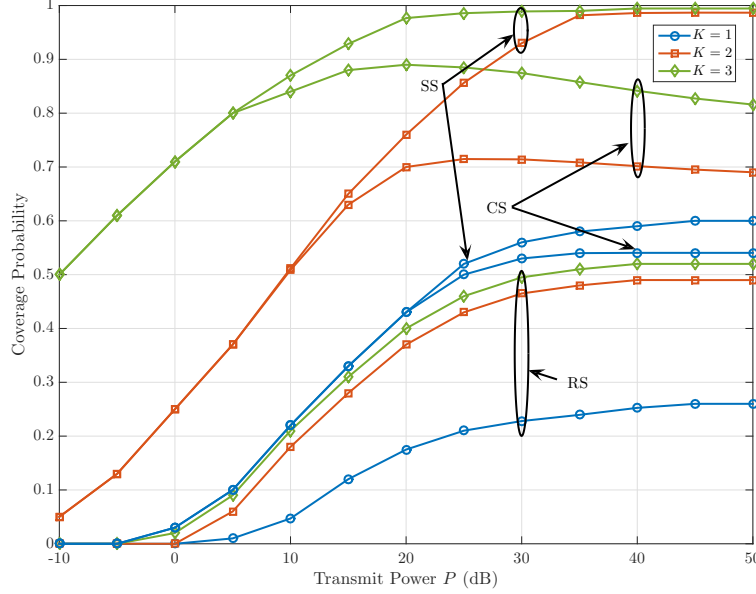


Fig. 5: Coverage probability versus transmit power for different numbers of tiers; $\lambda_1 = 5 \times 10^{-5}$, $\lambda_2 = 3\lambda_1$, $\lambda_3 = 4\lambda_1$, $P_1 = 3P$ dB, $P_2 = 2P$ dB, $P_3 = P$ dB, and $T = 0$ dB.

the number of network tier increases, the coverage performance improves. This observation has been expected, since as the number of network tier increases, the number of associated BSs with the users increases. As a result, the probability of a user to communicate with a BS that provides higher coverage performance is increased, thus the network performance improves. In addition, as it can be seen in Fig. 5, CS and SS schemes outperform the RS scheme independently of the transmit power value. In high and moderate transmit power values, the SS scheme outperforms the CS scheme, while in low transmit power values, their difference in terms of coverage performance is negligible. Additionally, it is clear from the plot that the coverage probability for all pre-selection policies converges to a constant value for high transmission powers. This behavior of coverage performance is based on the fact that as the transmission power of the network's nodes increases, the noise in the network becomes negligible.

Fig. 6 illustrates the importance of the deployment of sectorized antennas for mmWave networks in order to mitigate the negative effects caused by the blockages on the network performance. For each pre-selection policy, we plot the coverage probability versus the blockage constant and the main lobe gain of sectorized antennas. It can be easily observed that, as the blockage density increases, the network performance decreases independently from the adopted policy. As mentioned before, for high blockage densities, the communication of the users with LOS BSs becomes impossible and thus the coverage probability significantly decreases. In

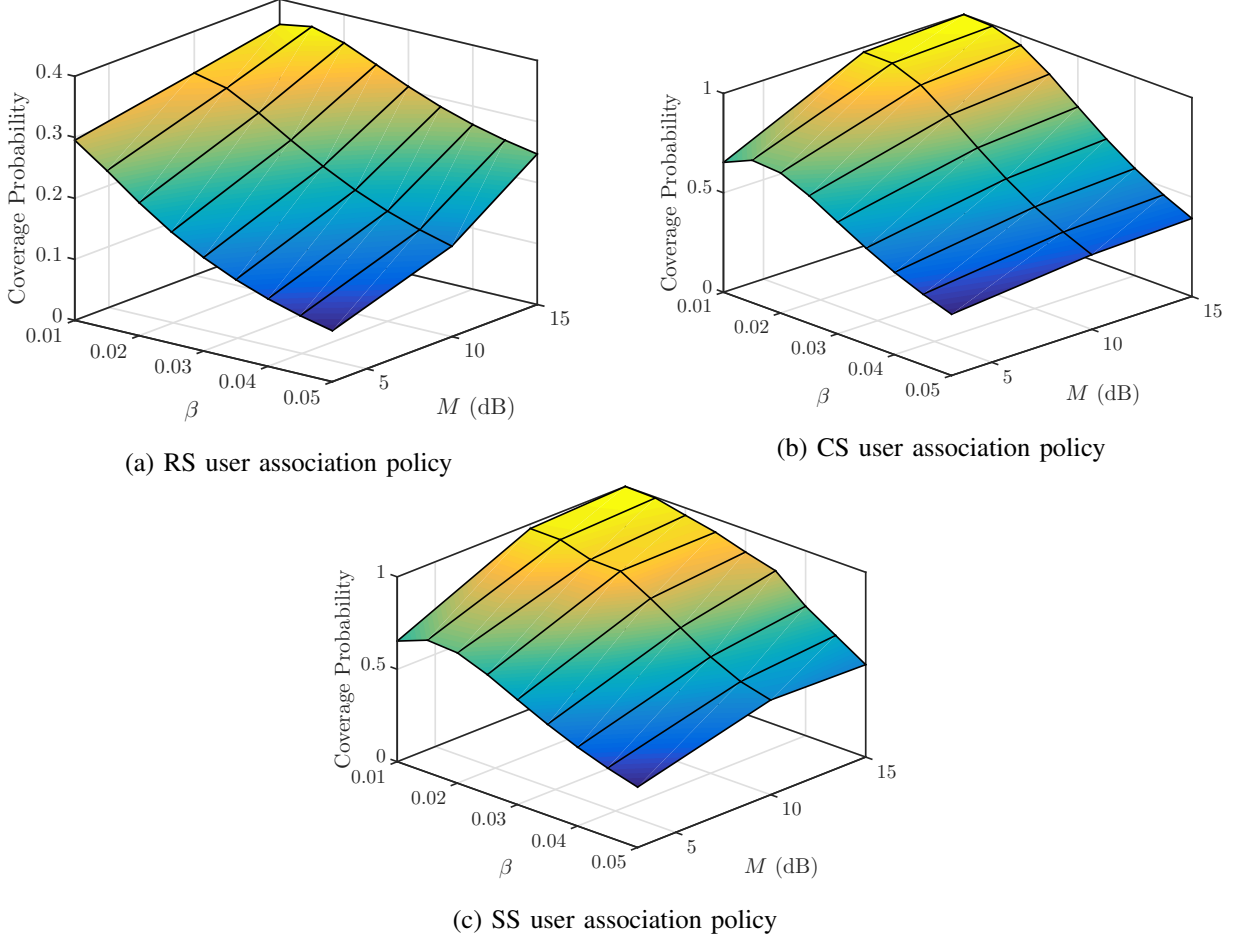


Fig. 6: Coverage probability versus blockage constant and main lobe gain; $T = 0$ dB.

addition, by narrowing the antenna's main lobe beamwidth, the coverage performance increases. This observation was expected, since by narrowing the main lobe beamwidth, the multi-user interference from interfering BSs is reduced and the observed SINR increases. Hence, it can be easily observed that, while the density of the blockages is increasing, in order to prevent a decrease in the network performance, the antenna's beamwidth should be narrowed.

In Fig. 7, we plot the additional achieved gain in terms of coverage probability versus the maximum number of cancellations and the SINR threshold. It can be seen that, the coverage probability sharply decreases with N and by increasing the SINR threshold. Specifically, by using the SIC scheme, a considerable improvement on the success probability is observed for SINR threshold values lower than 2 dB, whilst the improvement of the network performance is negligible for higher SINR threshold values. Furthermore, Fig. 7 shows that the achieved gain through the cancellation of the strongest interferer, is significantly larger than the gains achieved through the cancellation of higher order interferers. This was expected, due to the fact that by

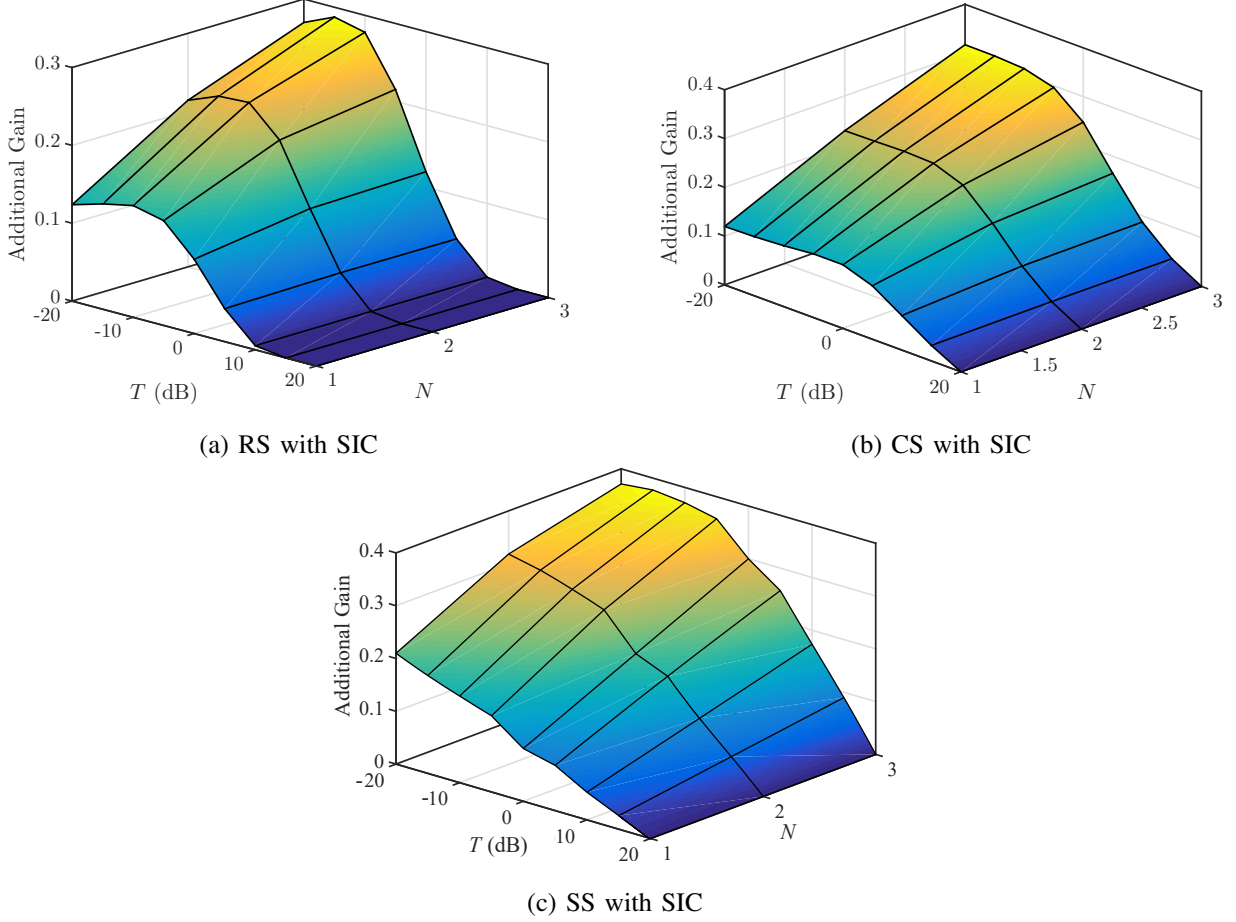


Fig. 7: Additional gain versus SINR threshold and number of maximum interfering BS cancelations.

decoding and subtracting the strongest interfering signal, the users face a noticeable weaker interference resulting in the improvement of observed SINR.

VII. CONCLUSION

In this paper, we proposed a novel low-complexity BS selection scheme in the context of next-generation cellular networks. We assumed that the users and the BSs are equipped with sectorized antennas and the users have the ability to perform SIC. We evaluated the achieved network performance by using our proposed technique in the context of three pre-selection policies that are based on: 1) the Euclidean distance, 2) the averaged received signal power, and 3) random selection. The coverage probability performance of our proposed technique was derived in analytical expressions for the case of Nakagami fading and the impact of blockage density, antenna directionality and number of network tiers has been discussed. Finally, aiming

to further boost the achieved performance, a SIC mechanism has been integrated at the user's side to mitigate strong interference terms for the special case of Rayleigh fading. **We have shown that the proposed BS selection scheme outperforms conventional CoMP schemes and ensures full diversity gain when the SS policy is employed.** A future extension of this work is the consideration of a distance-based power control to handle the effects of multi-user interference.

APPENDIX A

PROOF OF LEMMA 1

The intensity measure of LOS BSs is $\Lambda(r) = \frac{2\pi\lambda}{\beta^2} (1 - \exp(-\beta r)(1 + \beta r))$ and so their density is given by $\lambda(r) = d\Lambda(r)/dr$. Now, the distribution of the distance R to the closest LOS BS and the probability distribution function of R are given by [12, Theorem 8]

$$\mathbb{P}[R > r] = \exp\left(-\frac{2\pi\lambda}{\beta^2} (1 - \exp(-\beta r)(1 + \beta r))\right),$$

and

$$f_\Phi(r) = 2\pi\lambda r \exp\left(-\beta r - \frac{2\pi\lambda}{\beta^2} (1 - \exp(-\beta r)(1 + \beta r))\right),$$

respectively. The distance distributions are the same for any tier k since the network tiers are mutually independent. Therefore, we write $f_{\Phi_k}(r_k)$ for the distance distribution of the network tier k and hence, the joint distance distribution is given by the product of the distance distributions of all the network tiers.

APPENDIX B

PROOF OF THEOREM 1

Using the BSS technique as described before, the instantaneous coverage probability of the user where the link's status with its associated BS is ℓ , can be written as

$$\mathcal{P}_k^*(T \mid \ell, r_{u_k}^*) = \mathbb{P}\left[\frac{G_0 P_k h_{u_k}^* r_{u_k}^{*-a_\ell}}{\sigma^2 + I} \geq T\right] = 1 - \mathbb{P}\left[h_{u_k}^* < \frac{T r_{u_k}^{a_\ell}}{G_0 P_k} (\sigma^2 + I)\right]. \quad (44)$$

where $h_{u_k}^*$ is a gamma distributed random variable with parameter ν_ℓ . To overcome the difficulty on Nakagami fading, Alzer's Lemma [36] on the CCDF of a gamma random variable with integer parameter can be applied. This relates the CDF of a gamma random variable into a weighted sum of the CDFs of exponential random variables. Hence, we can bound expression (44) as

$$\mathcal{P}_k^*(T \mid \ell, r_{u_k}^*) < 1 - \mathbb{E}_{r,I} \left[\left(1 - \exp\left(-\frac{\eta_\ell T r_{u_k}^{a_\ell}}{G_0 P_k} (\sigma^2 + I)\right) \right)^{\nu_\ell} \right]$$

$$= \sum_{\xi=1}^{\nu_\ell} (-1)^{\xi+1} \binom{\nu_\ell}{\xi} \mathbb{E}_I \left[\exp \left(-\frac{\eta_\ell \xi T r_{u_k^*}^{a_\ell}}{G_0 P_k} (\sigma^2 + I) \right) \right], \quad (45)$$

where expression (45) is derived with the use of Alzer's Lemma [36] and $\eta_\ell = \nu_\ell(\nu_\ell!)^{-1/\nu_\ell}$. Based on the independence between network tiers, this allows us to use of the superposition theorem from stochastic geometry [33]. We further thin Φ based on the random antenna gain. Essentially, we can now view the interference, as

$$I = \sum_{i=1}^K \sum_G \sum_\ell I_i(v | G, \ell)$$

where I_i represents the interference caused by the BSs that are in $\ell \in \{\text{L}, \text{N}\}$ with the user, have link gain $G \in \{M^2, Mm, m^2\}$ and belong in network tier i . In essence, each expectation is the Laplace transform of the associated sub-PPP, $\mathcal{L}_{I_i}(s_\ell | G, \ell)$ where $s_\ell = \frac{\eta_\ell \xi T r_{u_k^*}^{a_\ell}}{G_0 P_k}$ and each of these Laplace transforms are multiplied together. Therefore, (45) can be rewritten as,

$$\mathcal{P}_k^*(T | \ell, r_{u_k^*}) < \sum_{\xi=1}^{\nu_\ell} (-1)^{\xi+1} \binom{\nu_\ell}{\xi} \exp(-s_\ell \sigma^2) \prod_{i=1}^K \prod_G \prod_\ell \mathcal{L}_{I_i}(s_\ell | G, \ell), \quad (46)$$

Using stochastic geometry tools, and specifically the probability generating functional of a PPP [33], we can analytically represent the Laplace transform for the interference I_i of the associated sub-PPP as

$$\mathcal{L}_{I_i}(s_\ell | G, \ell) = \exp \left(-p_G \int_{r_{u_i^*}}^{\infty} (1 - \mathbb{E}_h [\exp(-s_\ell G P_i h v^{-a_\ell})]) \lambda_i^\Pi(v | \ell) dv \right), \quad (47)$$

where for the considered pre-selection policy $\Pi \in \{\text{CS}, \text{SS}, \text{RS}\}$, $\lambda_i^\Pi(v | \ell)$ denotes the density of the BSs of which the link with the user is in a status ℓ and $\mathbb{E}_h[\exp(-xh)]$ corresponds to the MGF of the gamma random variable h with integer parameter ν , and is given by $(1+x)^{-\nu}$.

Thus, the Laplace interference function of the associated sub-PPP is given as

$$\mathcal{L}_{I_i}(s_\ell | G, \ell) = \exp \left(-p_G \int_{r_{u_i^*}}^{\infty} \left(1 - \left(1 + \frac{s_\ell G P_i v^{-a_\ell}}{\nu_\ell} \right)^{-\nu_\ell} \right) \lambda_i^\Pi(v | \ell) dv \right). \quad (48)$$

Thus, the Laplace transform of interference function is given by

$$\mathcal{L}_I(s_\ell) = \prod_{i=1}^K \prod_\ell \prod_G \mathcal{L}_{I_i}(s_\ell | G, \ell) \quad (49)$$

Finally, by substituting the Laplace interference function, into the conditional coverage probability expression (46); and by un-conditioning the derived expression with the appropriate joint distance distribution, we conclude to the desired expression.

APPENDIX C

PROOF OF REMARK 1

Based on the assumptions in Section IV-A for the case where $\beta \rightarrow 0$, the interference at the user is caused only by the side-lobes of the BSs (since $M \rightarrow \infty$) and so the gain of the interfering links is m^2 and $p_{m^2} = 1$, $p_{M^2} = p_{Mm} = 0$. Then, as we assume the interfering links do not experience fading, the Laplace transform in (47) can be written as

$$\mathcal{L}_{I_i}(s_L | m^2, L) = \exp \left(- \int_{r_{u_i}^*}^{\infty} \left(1 - \exp \left(- \frac{s_L m^2 P_i}{v^{a_L}} \right) \right) \lambda_i^{\text{CS}}(v | L) dv \right), \quad (50)$$

Now, for the case $\beta \rightarrow 0$, we have $\lambda_i^{\text{CS}}(r | L) = 2\pi\lambda_i r$ and so (50) is simplified to

$$\mathcal{L}_{I_i}(s_L | m^2, L) = \exp \left(\pi\lambda_i \left(r_{u_i}^2 + \frac{2}{a_L} (m^2 P_i s_L)^{\frac{2}{a_L}} \left(\Gamma \left[-\frac{2}{a_L} \right] - \Gamma \left[-\frac{2}{a_L}, \frac{s_L m^2 P_i}{r_{u_i}^{a_L}} \right] \right) \right) \right), \quad (51)$$

where $s_L = \frac{\eta_L \xi T r_{u_k}^{a_L}}{G_0 P_k}$, $\eta_\ell = \nu_\ell (\nu_\ell!)^{-1/\nu_\ell}$ and (51) follows from [37, 3.326.3]. Then, as the network is ultra-dense, we can assume that the interference-free area around the user is negligible i.e., $r_{u_i}^* \rightarrow 0$. Hence, (51) can be further simplified to

$$\mathcal{L}_{I_i}(s_L | m^2, L) = \exp \left(-\pi (m^2 P_i s_L)^{\frac{2}{a_L}} \lambda_i \Gamma \left[1 - \frac{2}{a_L} \right] \right), \quad (52)$$

which follows from the identities $\Gamma[1 - a] = -a\Gamma[-a]$ and $\lim_{x \rightarrow \infty} \Gamma[a, x] \rightarrow 0$. Thus, by substituting the above expression to (13), (15) follows from [37, 3.326.2]. By following similar steps, we can derive the network performance for the case where $\beta \rightarrow \infty$.

APPENDIX D

PROOF OF LEMMA 2

The process $\Psi = \cup_{k=1}^K \Psi_k$ is a non-homogeneous PPP with density $\lambda(\gamma) = \sum_{k=1}^K \lambda_k(\gamma)$. Using the transformation $r = (\gamma P_k)^{1/a_L}$ and the mapping theorem [33], the intensity measure of each network tier $k \in \{1, \dots, K\}$ for LOS and NLOS BSs are given by

$$\begin{aligned} \Lambda_k([0, (\gamma P_k)^{1/a_L}] | L) &= \int_0^{(\gamma P_k)^{1/a_L}} 2\pi\lambda_k x \exp(-\beta x) dx \\ &= \frac{2\pi\lambda_k}{\beta^2} (1 - \exp(-\beta(\gamma P_k)^{1/a_L}) (1 + \beta(\gamma P_k)^{1/a_L})), \end{aligned}$$

and

$$\Lambda_k([0, (\gamma P_k)^{1/a_N}] | N) = \int_0^{(\gamma P_k)^{1/a_N}} 2\pi\lambda_k x (1 - \exp(-\beta x)) dx$$

$$= \pi \lambda_k (\gamma P_k)^{1/a_N} - \frac{2\pi \lambda_k}{\beta^2} \left(1 - \exp \left(-\beta (\gamma P_k)^{1/a_N} \right) \left(1 + \beta (\gamma P_k)^{1/a_N} \right) \right),$$

respectively. Then, $\lambda_k((\gamma P_k)^{1/a_\ell} | \ell) = d\Lambda_k([0, (\gamma P_k)^{1/a_\ell}] | \ell) / d\gamma$ where $\ell \in \{L, N\}$, gives the density of the BSs. Therefore, the distance distribution of the tier k is given by

$$f_{\Psi_k}((\gamma P_k)^{1/a_\ell}) = \lambda_k((\gamma P_k)^{1/a_\ell}) \exp \left(-\Lambda_k[0, (\gamma P_k)^{1/a_\ell}] \right), \quad (53)$$

and the joint distance distribution is given by the product of the individual distance distributions due to the independence of the tiers.

REFERENCES

- [1] C. Skouroumounis, C. Psomas, and I. Krikidis, "Low-complexity base station cooperation for mmWave heterogeneous cellular networks," in *Proc. IEEE Global Commun. Conf.*, Washington, DC, Dec. 2016, pp. 1–6.
- [2] A. Ghosh, R. Ratasuk, B. Mondal, N. Mangalvedhe, and T. Thomas, "LTE-advanced: Next generation wireless broadband technology," *IEEE Wireless Commun.*, vol. 17, pp. 10–22, Jun. 2010.
- [3] B. Yin, S. Abu-Surra, G. Xu, T. Henige, E. Pisek, Z. Pi, and J. R. Cavallaro, "High-throughput beamforming receiver for millimeter wave mobile communication," in *Proc. Consumer Commun. Netw. Conf.*, Las Vegas, NV, Jan. 2014, pp. 537–543.
- [4] R. W. Heath, N. Gonzalez-Prelcic, S. Rangan, W. Roh, and A. M. Sayeed, "An overview of signal processing techniques for millimeter wave MIMO systems," *IEEE J. Select. Signal Proc.*, vol. 10, no. 3, pp. 436–453, Apr. 2016.
- [5] T. S. Rappaport, R. W. Heath, R. C. Daniels, and J. N. Murdock, *Millimeter wave wireless communications*, Prentice Hall, 2014.
- [6] H. S. Dhillon, R. K. Ganti, F. Baccelli, and J. G. Andrews, "Modeling and analysis of K-tier downlink heterogeneous cellular networks," *IEEE Trans. Wireless Commun.*, vol. 30, pp. 550–560, Apr. 2012.
- [7] L. Wu, Y. Zhong, and W. Zhang, "Spatial statistical modeling for heterogeneous cellular networks-an empirical study," in *Proc. IEEE Veh. Technol. Conf.*, Seoul, Korea, May 2014, pp. 1–6.
- [8] D. Lee, "Coordinated multipoint transmission and reception in LTE-Advanced: Deployment scenarios and operational challenges," *IEEE Commun. Mag.*, vol. 50, pp. 148–155, Feb. 2012.
- [9] J. G. Andrews, S. Buzzi, W. Choi, S. V. Hanly, A. Lozano, A. C. K. Soong, and J. C. Zhang, "What will be 5G be?," *IEEE J. Select. Areas Commun.*, vol. 32, pp. 1065–1082, Jun. 2014.
- [10] R. Tanbourgi, S. Singh, J. G. Andrews, and F. K. Jondral, "A tractable model for noncoherent joint-transmission base station cooperation," *IEEE Trans. Wireless Commun.*, vol. 13, pp. 4959–4973, Sept. 2014.
- [11] G. Nigam, P. Minero, and M. Haenggi, "Coordinated multipoint joint transmission in heterogeneous networks," *IEEE Trans. Commun.*, vol. 62, pp. 4134–4146, Oct. 2014.
- [12] T. Bai, R. Vaze, and R. W. Heath, "Analysis of blockage effects on urban cellular networks," *IEEE Trans. Wireless Commun.*, vol. 13, pp. 5070–5083, Jun. 2014.
- [13] C. Skouroumounis, C. Psomas, and I. Krikidis, "Low complexity base station cooperation in cellular networks with blockages," in *Proc. IEEE Wireless Commun. Netw. Conf.*, Doha, Qatar, Apr. 2016, pp. 1381–1386.
- [14] M. Akdeniz, Y. Liu, M. Samimi, S. Sun, S. Rangan, T. Rappaport, and E. Erkip, "Millimeter wave channel modeling and cellular capacity evaluation," *IEEE J. Select. Areas Commun.*, vol. 32, pp. 1164–1179, Jun. 2014.
- [15] P. Wang, Y. Li, L. Song, and B. Vucetic, "Multi-gigabit millimeter wave wireless communications for 5G: from fixed access to cellular networks," *IEEE Comms. Magazine*, vol. 53, pp. 168–178, Jan. 2015.

- [16] N. A. Muhammad, P. Wang, Y. Li, and B. Vucetic, "Analytical model for outdoor millimeter wave channels using geometry-based stochastic approach," *IEEE Trans. Veh. Technol.*, vol. 66, no. 2, pp. 912–926, Feb. 2017.
- [17] J. G. Andrews, T. Bai, M. Kulkarni, A. Alkhateeb, A. Gupta, and R. W. Heath, "Modeling and analyzing millimeter wave cellular systems," *IEEE Trans. Commun.*, vol. 65, no. 1, pp. 403–430, Jan. 2017.
- [18] D. Maamari, N. Devroye, and D. Tuninetti, "Coverage in mmWave cellular networks with base station cooperation," *IEEE Trans. Wireless Commun.*, vol. 15, pp. 2981–2994, Apr. 2016.
- [19] R. Ramanathan, J. Redi, C. Santivanez, D. Wiggins, and S. Polit, "Ad hoc networking with directional antennas: A complete system solution," *IEEE J. Select. Areas Commun.*, vol. 23, pp. 496–506, Mar. 2005.
- [20] S. Bellofiore, J. Foutz, R. Govindarajula, I. Bahceci, C. Balanis, A. Spanias, J. Capone, and T. Duman, "Smart antenna system analysis, integration and performance for mobile ad-hoc networks (MANETs)," *IEEE Trans. Ant. Propag.*, vol. 50, pp. 571–581, May 2002.
- [21] R. Choudhury, X. Yang, R. Ramanathan, and N. Vaidya, "On designing MAC protocols for wireless networks using directional antennas," *IEEE Trans. Mobile Computing*, vol. 5, pp. 477–491, May 2006.
- [22] P. Gupta and P. R. Kumar, "The capacity of wireless networks," *IEEE Trans. Inf. Theory*, vol. 46, pp. 388–404, May 2000.
- [23] A. Thornburg, T. Bai, and R. W. Heath, "Performance analysis of outdoor mmWave ad hoc networks," *IEEE Trans. Sign. Proc.*, vol. 64, pp. 4065–4079, Aug. 2016.
- [24] B. Tinyang and R. W. Heath, "Coverage and rate analysis for millimeter-wave cellular networks," *IEEE Trans. Wireless Commun.*, vol. 14, pp. 1100–1114, Feb. 2015.
- [25] E. Turgut and M. C. Gursoy, "Coverage in heterogeneous downlink millimeter wave cellular networks," in *Proc. IEEE Global Commun. Conf.*, Washington, DC, Dec. 2016, pp. 1–6.
- [26] X. Yu, J. Zhang, and K. B. Letaief, "Coverage analysis for dense millimeter wave cellular networks: The impact of array size," in *Proc. IEEE Wireless Commun. Netw. Conf.*, Doha, Qatar, Apr. 2016, pp. 1558–2612.
- [27] N. H. Mahmood, I. S. Ansari, G. Berardinelli, P. Mogensen, and K. A. Qaraqe, "Analysing self interference cancellation in full duplex radios," in *Proc. IEEE Wireless Commun. Netw. Conf.*, Doha, Qatar, Apr. 2016, pp. 1–6.
- [28] E. Bjrnson, L. Sanguinetti and M. Kountouris, "Deploying dense networks for maximal energy efficiency: small cells meet massive MIMO," *IEEE J. Select. Areas Commun.*, pp. 832–847, Apr. 2016.
- [29] G. Zhang and M. Haenggi, "The performance of successive interference cancellation in random wireless networks," *IEEE Trans. Inf. Theory*, vol. 60, pp. 6368–6388, Oct. 2014.
- [30] G. Zhang and M. Haenggi, "On decoding the k th strongest user in Poisson networks with arbitrary fading distribution," in *Proc. Asilomar Conf. Signals, Systems and Computers*, Pacific Grove, CA, May 2013, pp. 733–737.
- [31] G. Zhang and M. Haenggi, "Successive interference cancellation in downlink heterogeneous cellular networks," in *Proc. IEEE Global Commun. Conf.*, Atlanta, GA, Dec. 2013, pp. 730–735.
- [32] M. Wildemeersch, T. Q. Quek, M. Kountouris, A. Rabbachin, and C. H. Slump, "Successive interference cancellation in heterogeneous cellular networks," *IEEE Trans. Commun.*, vol. 62, pp. 2006–2021, Jun. 2014.
- [33] M. Haenggi, *Stochastic geometry for wireless networks*, in Cambridge, U.K.: Cambridge Univ. Press, 2012.
- [34] S. H. Park, O. Simeone, and S. Shamai, "Joint optimization of cloud and edge processing for fog radio access networks," *IEEE Trans. Wireless Commun.*, vol. 15, pp. 7621–7632, Nov. 2016.
- [35] Z. Yazdanshenasan, H. Dhillon, M. Afshang, and P. Chong, "Poisson hole process: Theory and applications to wireless networks," *IEEE Trans. Wireless Commun.*, vol. 15, pp. 7531–7546, Nov. 2016.
- [36] H. Alzer, "On some inequalities for the incomplete Gamma function," *Mathematics of Computation*, pp. 771778, 1997.
- [37] I. S. Gradshteyn and I. M. Ryzhik, *Table of integrals, series, and products*, in Elsevier, Academic Press, 2007.